

Analysis of blocking events from observations and ECHAM model simulations

By R. SAUSEN*, *Deutsche Forschungsanstalt für Luft- und Raumfahrt, Institut für Physik der Atmosphäre, Oberpfaffenhofen, D-82234 Weßling, Germany*, W. KÖNIG** and F. SIELMANN, *Meteorologisches Institut der Universität Hamburg, Bundesstraße 55, D-20146 Hamburg, Germany*

(Manuscript received 2 February 1994; in final form 24 October 1994)

ABSTRACT

A new objective routine for the identification of individual blocking events has been developed which is applicable to data sets of different horizontal resolution. It is based on the 500 hPa geopotential height anomalies with respect to a mean seasonal cycle. Three features of blocking are checked with this method: the intensity of the anomaly exceeding some threshold, a certain extension prescribed by a peripheral value of geopotential height, and a duration of at least 5 days. The routine is applied to ECMWF analyses and to climate simulations of the Northern Hemisphere, which were performed with the atmosphere model ECHAM3. In winter, the blocking statistics derived from the observations are in accord with the results of other identification techniques. In other seasons the differences are larger due to a different definition of blocking. It is shown that the model ECHAM3 simulates the observed two-dimensional frequency distribution of blocking events quite realistically.

1. Introduction

Blocking is usually defined as a mid-latitude anomalous flow pattern associated with a strong meridional wind component. Its horizontal extension ranges between the cyclonic and the planetary scale. A blocking event is either stationary or slowly migrating. Its lifetime usually amounts to several days. Especially in the Northern Hemisphere it is most frequently observed in distinct regions. The blocking pattern is characterized by a region of warm air with higher than ambient pressure. A split of the jet stream is found upstream. The associated pressure or geopotential height maximum tends to fluctuate in amplitude and width. The development and maintenance of blocking events is substantially influenced by small scale motions as inferred by studies on changes of resolution (Bengtsson, 1981; Tibaldi and Ji, 1983).

In order to study blocking phenomena in long time series of observed or modelled atmospheric circulation data objective procedures for identifying blocking events were developed. In previous publications three major characteristics were utilized for the identification of blocking events: first a split-up upper-air flow pattern, second a geopotential height maximum and third the properties of eddy fields related to the specific flow.

From a phenomenological point of view, the most striking feature of a blocking event is its characteristic flow split. Rex (1950) gave a comprehensive definition of blocking as an upper-air flow anomaly, expressed by a branching of the jet stream and a persistence over a certain time period of about 10 days. The persistence criterion, however, seems to be a too strong restriction, and was therefore often eliminated in further applications.

The identification of blocking events by a split westerly current is nowadays mainly utilized for the Southern Hemisphere (Noar, 1983). For each longitude the blocking index is evaluated from the

* Corresponding author.

** Present affiliation: Gustav-Siewerth-Akademie, Oberbierbronnen 1, D-79809 Weilheim, Germany.

differences of 500 hPa zonal wind at 45°S with that at 30°S and 60°S, respectively. Blocking situations are defined by positive values of this index. A shortcoming of this procedure is the specification of certain latitudes, which may be appropriate for present day climate, but which may fail in a different climate, e.g., in a climate with higher CO₂ concentration or a paleo climate, where the area of occurrence of blocking events might be shifted meridionally. Moreover, the analysis of the wind field is subject to more uncertainties and errors than the geopotential height.

From the original flow anomaly criteria by Rex equivalent conditions on the geopotential height field can be derived. In this connection a blocking event is defined as a height anomaly relative to a regional mean. The method is applied with several modifications in a number of recent studies (Hartmann and Ghan, 1980; Lejenäs and Økland, 1983; Mullen, 1986; Tibaldi and Molteni, 1990). The procedure of Lejenäs and Økland (1983) excels by its economical applicability to large datasets. It is applied to the Northern Hemisphere only. A split-up flow pattern is checked by a certain threshold for the meridional gradient of geopotential height. Further on it is investigated whether the criterion is fulfilled for a contiguous region of a valuable extension to avoid erroneous classification of small scale systems. A check on the duration of the feature is omitted. The method was improved by Tibaldi and Molteni (1990). A second gradient criterion to the north of the westerly flow maximum was introduced to exclude persistent circulation anomalies with a southerly displaced jet. These situations marginally fulfil the original criterion of Lejenäs and Økland. In a recent modification (Tibaldi et al., 1993) an additional criterion on the anomalies of geopotential height pentads is introduced in order to ensure the suspension of short-time fluctuations. The method was checked with observations and was found to render realistic results. Nevertheless, empirical parameters, like the latitude at which the meridional gradient is determined, become essential for this method. But these parameters hamper the applicability of the method to different climates.

The investigation of geopotential height maxima is certainly the most straightforward way of blocking identification. Elliot and Smith (1949) presented a rather simple procedure of objective

identification, which is easily applicable for automatical processing. They computed surface pressure anomalies from the climatological mean and counted the number of those grid points within certain regions, where the anomalies exceeded a certain threshold. The threshold should be exceeded for at least three days in order to specify a blocking situation. The dependence of this procedure on some arbitrary parameters, like the definition of a climate mean, the anomaly threshold, the critical grid point number, the duration of persistence, or even the selection of the blocking regions, hampered its further application.

An identification based on 500 hPa geopotential height field was proposed by Baur (1958). The study was confined to the Northern Hemisphere. A blocking event was identified if the geopotential height maximum was found north of 50°N and if it exceeded a certain reference value. However, not all of the observed blocking situations could be registered with these criteria. Thus, Baur also recognized a ridge as a blocking region, as long as a certain gradient on its west and east edges was discovered. The method avoids the problem of selection of a proper climate mean, but accepts the dependence on rather empirical thresholds.

From the lack of localized maxima as a tool for identification, methods of pattern comparison of surface pressure or geopotential height fields with standard cases were developed (Brezowsky et al., 1951; Sumner, 1954). But these phenomenological tools suffered from some arbitrariness, for example when a comparison with some climatological standard cases ("Grosswetterlagen") is involved as in Brezowsky et al., or when a coincidence of a cellular structure in 500 hPa geopotential height field and 500 over 1000 hPa relative topography charts is searched for as in Sumners study.

In the tradition of Elliot and Smith (1949) temporal anomalies were often utilized for automatical routines for the identification of blocking events (Charney et al., 1981; Dole and Gordon, 1983; Knox and Hay, 1984). Here the problem is to find a proper definition of the anomaly. Charney et al. calculated the anomalies by subtracting a mean annual cycle based on an ensemble mean of grid points. The anomalies should exceed a certain margin and last for a given time period to distinguish a blocking situation. The margins were fitted to a resolution of 5° × 5° by an inspection of significant preferences for the occurrence of

anomalies of certain magnitudes. A further specification of the criterion with regard to the extension of the patterns and their kinematic structure seems to be essential. Dole and Gordon (1983) applied a similar procedure to select persistent and intense geopotential height anomalies which resemble blocking situations. They compared the performance of their method for different anomaly margins and persistence times and contrasted the frequencies of positive and negative persistent anomalies. For durations of 5 days and more the probability of an anomaly to last at least one more day is almost constant. A difference of 150 gpm turned out to be a reasonable margin to identify a blocking situation. Negative anomalies satisfying the analogous thresholds are less frequent than blocking events.

Another approach to blocking identification by Knox and Hay (1984) uses anomalies in 5-day averaged height fields. The height threshold for blocking cases is determined as a function of latitude and season. For successive pentades a distance criterion is introduced. If two anomalies in successive pentades are less distant than a certain margin, they are identified as one slowly moving blocking event.

Among the more recent objective identification techniques Mullens (1986, 1987) method has to be mentioned, which utilizes some of the earlier experiences of Elliott and Smith (1949) and Hartmann and Ghan (1980). Blocking is defined as a continuous occurrence of a geopotential height anomaly of at least 150 gpm in 500 hPa for a period of at least 7 days. The anomaly was calculated respective to areal means of certain sectors of the latitude belt between 50°N and 60°N. To remove fast-propagating transient disturbances with periods of less than 5 days the input data were smoothed by a weak low-pass filter (Blackmon et al., 1986). The advantage of Mullens method is its independence of data resolution, but the problem of arbitrariness concerning the choice of the margins and the selection of the sectors still remains. This shortcoming can probably never be totally ruled out in objective identification methods.

As mentioned in the beginning of the introduction, also the eddy field can be used as an indicator of blockings. Sumner (1959) noted that the persistence of blocking is associated with the absorption of cyclonic and anticyclonic eddy vorticity in

the poleward and equatorward parts, respectively. Blackmon et al. (1986) used low-pass filtered geopotential height fields to identify blockings. The major weakness of this method lies in its inability to distinguish between blockings highs and cut-off lows. The results render a rich variety of different slowly evolving features included in the filter interval, which cannot be attributed to the blocking scale exclusively.

From the critical review of the different methods of blocking identification, two general inferences on the concept of objective pattern recognition can be drawn: first, the procedure should be independent of the shape of the pattern. Secondly, the computational expenditure should be balanced by the efficiency of its application. The first condition includes that the method should be based on general criteria which are independent of data resolution. A certain amount of arbitrariness in the choice of margins and thresholds has to be put up with. Nevertheless, the number of empirical parameters should be reduced to a minimum. It is evident from the review of literature that three characteristic measures are essential for blocking identification: not only the frequency of intense positive anomalies of geopotential height, but also its duration and its spatial extension have to be considered.

For the validation of atmospheric models of various horizontal resolutions and for analysing climate change simulations we would like to use a blocking identification method which does not have certain shortcomings of the methods reviewed above. As we are interested in identifying individual blocking events the technique of time filtering eddy vorticity field cannot be used, despite its computational efficiency. The methods based on certain meridional gradients of the geopotential height field or the zonal velocity field suffer from the choice of a pre-selected latitude, which makes their use in a changed climate questionable. These methods provide the zonal distribution of blocking, the two dimensional structure of the blocking frequency field cannot be obtained (as is possible in the case of low-pass filtering of eddy fields). Thus we have decided to choose a method which is an extension of Mullens (1986, 1987) method to the Northern Hemisphere or potentially to the globe as a whole. The time filtering can be skipped, and the selection of sectors is not necessary either.

Our method is described in Section 2, with parameters suitable for the Northern Hemisphere. In order to demonstrate its performance our method is applied to ECMWF analyses and to simulations with the atmosphere general circulation model ECHAM in T21 and T42 resolution (Section 3). A comparison of our results to the blocking distribution based on the frequently used method by Tibaldi and Molteni (1990) is performed. In the summary (Section 4) both the questions of the blocking phenomenon as a climate indicator and as a tool for model validation will be dealt with.

2. Method

To identify individual blocking events we base our method on the 500 hPa geopotential height field. First the annual cycle has to be removed and the time series of data has to be detrended (e.g., a trend may arise due to climate change in a global warming experiment). Second the anomaly field is inserted in a routine identifying contiguous regions, where the field exceeds a threshold.

2.1. Removal of annual cycle and trend

At each grid point we calculate an anomaly $z'(\lambda, \varphi, t)$ of the 500 hPa geopotential height field

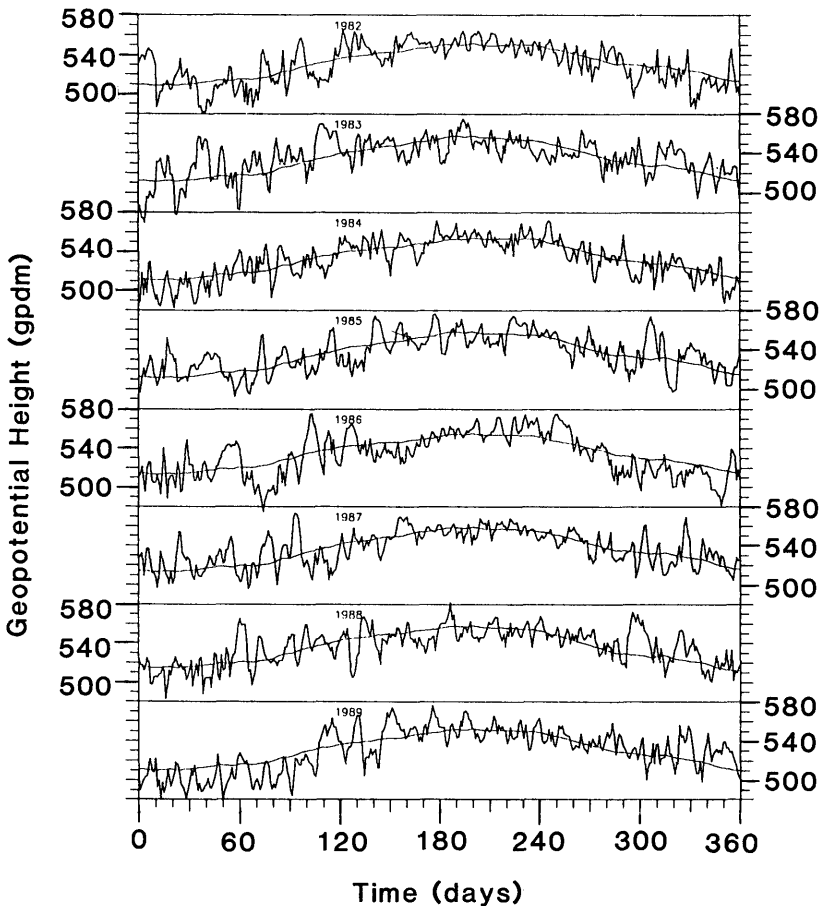


Fig. 1. Time series of the 500 hPa geopotential height z of ECMWF analyses at grid point (45°W , 60°N) from 1 January 1982 until 31 December 1989. Daily values of z (thick line), and the sum of the running annual mean plus the mean annual cycle $\bar{z} + \hat{z}$ (thin line) are plotted.

$z(\lambda, \varphi, t)$, where t is the number of the time step in the case of model data, or the number of the field in the case of observational data. By definition the number of the first field is $t = 1$. In the following, the spatial subscripts λ (longitude) and φ (latitude) are omitted for the sake of simplification. Let us assume that the length of data set is K years and that the grid length of the time grid is Δt . N is the mean number of data points per year, thus $1 \leq t \leq K \cdot N$. In the case of ECHAM model simulations, which we will analyse later, each model year consists of 12 months with 30 days, i.e., for model data we have $N \Delta t = 360$ days.

Then we proceed in the following way (see also Figs. 1, 2):

- (1) We determine a running annual mean

(with special treatment of the beginning and the end of the time series):

$$\bar{z}(t) = \begin{cases} \frac{1}{N+1} \sum_{t-N/2 \leq \tau \leq t+N/2} z(\tau) & \text{for } \frac{1}{2}N < t < KN - \frac{1}{2}N \\ \bar{z}\left(\frac{1}{2}N + 1\right) & \text{for } 1 \leq t \leq \frac{1}{2}N \\ \bar{z}\left(KN - \frac{1}{2}N - 1\right) & \text{for } KN - \frac{1}{2}N \leq t \leq KN. \end{cases} \quad (1)$$

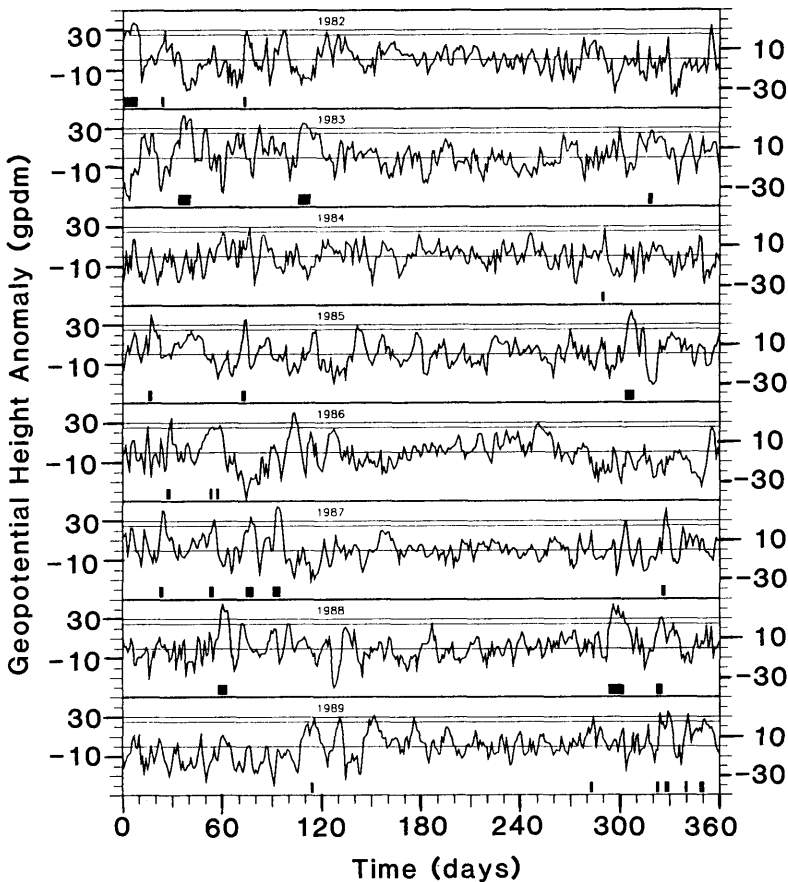


Fig. 2. Time series of the 500 hPa geopotential height anomaly z' of ECWMF analysis at grid point (45° W, 60° N) from 1 January 1982 to 31 December 1989. The thin horizontal lines indicate the margins of 250 gpm and 300 gpm, respectively. Black bars show situations where a blocking event is located at this grid point.

(2) We calculate a running monthly mean z^* of the anomaly relative to \bar{z} . If M is the number of data points per month*, we define:

$$z^*(t) = \begin{cases} \frac{1}{M+1} \sum_{t-M/2 \leq \tau \leq KN-M/2} (z(\tau) - \bar{z}(\tau)) & \text{for } \frac{1}{2}M < t < KN - \frac{1}{2}M \\ z\left(\frac{1}{2}M + 1\right) & \text{for } 1 \leq t \leq \frac{1}{2}M \\ z\left(KN - \frac{1}{2}M - 1\right) & \text{for } KN - \frac{1}{2}M \leq t \leq KN. \end{cases} \quad (2)$$

(3) The mean annual cycle \hat{z} is calculated for $1 \leq \tau \leq N$:

$$\hat{z}(\tau) = \frac{1}{K} \sum_{i=1}^K z^*(N(i-1) + \tau). \quad (3)$$

For a selected grid point of observations Fig. 1 shows the unmanipulated time series $z(t)$ and the running annual mean plus the mean annual cycle $\bar{z}(t) + \hat{z}(\tau)$.

(4) A preliminary anomaly is determined by removing the mean annual cycle and the running annual mean, i.e., for $t = N(i-1) + \tau$ we calculate

$$z(t) - \bar{z}(t) - \hat{z}(\tau). \quad (4)$$

(5) After removing the long-term temporal mean of this quantity we obtain the desired anomaly:

$$z'(t) = z(t) - \bar{z}(t) - \hat{z}(\tau) - \langle z - \bar{z} - \hat{z} \rangle, \quad (5)$$

where for any function $g(t)$ the temporal mean is defined by

$$\langle g \rangle = \frac{1}{KN} \sum_{1 \leq t \leq KN} g(t). \quad (6)$$

* In order to simplify the procedure we choose also for analyses M such that $M \Delta t = 30$ days.

Fig. 2 shows the anomalies z' for the selected grid point of Fig. 1.

Fig. 3a shows a Hovmöller diagram at 60° N of the anomaly z' for an arbitrarily selected 180 days period taken from an annual cycle control run that was performed with the general circulation model ECHAM2/T42 (shown are the first 6 months of model year 17)**. Only the 250 and 300 gpm isolines are plotted. Areas with $z' \geq 300$ gpm are shaded.

2.2. Identifying individual blocking events

The anomaly z' is now inserted into our routine for detecting blocking events. The criteria of the objective pattern recognition method are based on the three properties of blocking mentioned in the introduction, i.e., an anomaly exceeding a certain margin, a duration longer than some period and a variable spatial extension. This is achieved by a two-step procedure:

(1) In the three-dimensional space-time domain $(\lambda, \varphi$ and $t)$ we search for contiguous areas (definition below) with $z' \geq 300$ gpm that exist for at least 5 days.

Given the grid lengths $\Delta\lambda, \Delta\varphi$ and Δt , two grid points $(\lambda_1, \varphi_1, t_1)$ and $(\lambda_2, \varphi_2, t_2)$ are called *adjacent* if $|\lambda_1 - \lambda_2| \leq \Delta\lambda, |\varphi_1 - \varphi_2| \leq \Delta\varphi$ and $|t_1 - t_2| \leq \Delta t$. Two grid points $(\lambda_1, \varphi_1, t_1)$ and $(\lambda_2, \varphi_2, t_2)$ belong to the same *contiguous* area, if they are adjacent or if a chain of m grid points $(\lambda_3, \varphi_3, t_3), (\lambda_4, \varphi_4, t_4), \dots, (\lambda_{m+2}, \varphi_{m+2}, t_{m+2})$ exists, such that

$$(\lambda_1, \varphi_1, t_1) \text{ is adjacent to } (\lambda_3, \varphi_3, t_3),$$

$$(\lambda_3, \varphi_3, t_3) \text{ is adjacent to } (\lambda_4, \varphi_4, t_4),$$

...

$$(\lambda_{m+2}, \varphi_{m+2}, t_{m+2}) \text{ is adjacent to } (\lambda_2, \varphi_2, t_2).$$

(2) The detected areas are then contiguously extended by those points with $z' \geq 250$ gpm, such

** At this place, the origin of the data set is of no importance, any 500 hPa data set containing blocking events could serve as an example. We will return to that run in Section 3, where also more details will be given.

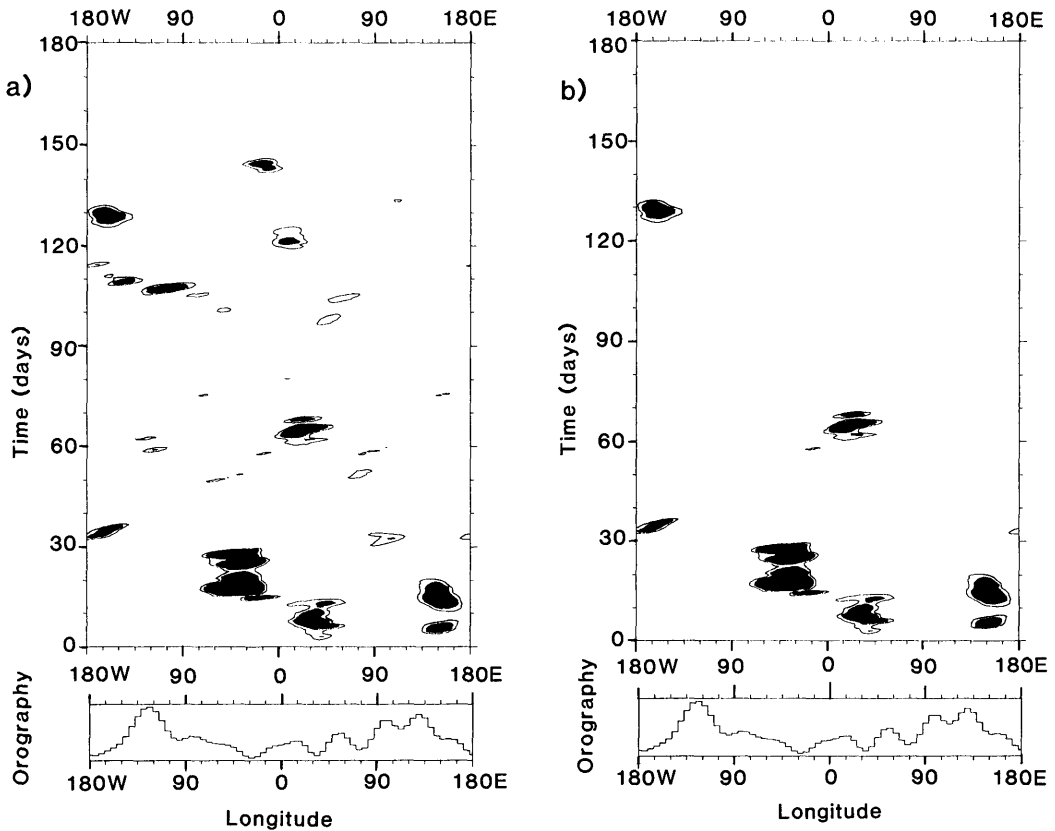


Fig. 3. (a) Hovmöller diagram of geopotential height anomalies z' along 60°N for a 180 days period of a ECHAM3/T42 model simulation. Occurrences of $z' \geq 300$ gpm are shaded. Further on, an isoline at $z' \geq 250$ gpm is added. The small sketch below illustrates the orography. (b) Same as (a), but after application of the blocking criteria.

that the original area is embedded in a new contiguous area with $z' \geq 250$ gpm.

Applying these selection procedure transforms Fig. 3a into Fig. 3b. In our test example, the major blocking activity is found in January, over the western Atlantic, over Europe and over the eastern Pacific. The most extensive blocking event, which also has the longest duration, is found over the western Atlantic. Approaching the summer season the blocking activity decreases substantially. The short-time positive anomalies, most of them over the Pacific, do not pass the duration threshold of 5 days. Thus only the marked patterns in the winter half year are retained, a behaviour well-known from observations. In Fig. 2 the detected blocking events of the observational data are marked by bars.

Our method will not only detect blocking events which are stationary, but also recognize events that slowly move both in zonal and/or meridional direction. In this respect our method is different to the method previously applied by Trenberth and Mo (1985) or Bates and Meehl (1986), who did not regard any spatial shift or spatial correlations. Our method is independent of any preselected latitude; thus it will also work in the case of a changed climate, where the latitudinal position of blocks may be different from the present day position.

Some arbitrariness lies in the selection of the thresholds of 5 days, and 250 and 300 gpm. However, experiments proved that our method is not very sensitive to the minimum duration threshold. Normally, a blocking event that exists 5 days will also exist 6 or 7 days. A greater sensitivity

is found with respect to the thresholds for the geopotential height anomaly. The values of 300 and 250 gpm, resp., were empirically chosen by a comparison with synoptically analysed 500 hPa maps.

Our thresholds for the geopotential height anomaly are higher than the threshold suggested by Shukla and Mo (1983) for the Northern Hemisphere winter. On the other hand we use a shorter time threshold and take into account also moving pattern and thus detect some additional events. In contrast to some other authors (Shukla and Mo, 1983; Trenberth and Mo, 1985) we prefer thresholds that are seasonally independent. Of course, this drastically reduces the number of detected events if we compare with the results of Shukla and Mo (1993) or Bates and Meehl (1986). One might think of different thresholds for the Southern Hemisphere, but we will not discuss this hemisphere in the current paper.

3. Application

In this section, we demonstrate the performance of our method for identifying blocking events by applying it to several Northern Hemisphere data sets, observational data and atmosphere model output. At the same time a validation of the atmospheric general circulation model ECHAM is made. Finally we apply the method to a model simulation with a warmer climate (due to a rise of atmospheric CO₂ content).

3.1. Data

The data inserted into our identification method are either observations or they originate from various ECHAM model simulations (see Table 1 for an overview). As observations we take ECMWF analyses of the period 1982–1989. The resolution was truncated to T42 which corresponds to a horizontally homogeneous resolution of approximately 4.3° (480 km). The data were then transformed to a Gaussian grid with approximately 2.8° horizontal resolution.

The model data were generated by the Hamburg spectral atmosphere general circulation model ECHAM, either in uncoupled mode with prescribed sea surface temperature (SST) or in the coupled mode, where the SST is interactively simulated by an ocean general circulation model. The ECHAM model has been developed on the

basis of the numerical weather prediction model of ECMWF. Prognostic variables are vorticity, divergence, temperature, (logarithm of) surface pressure, humidity and cloud water (ice and water phase). The model contains parameterisations of radiation, cloud formation and precipitation, convection, and vertical and horizontal diffusion. Land surface processes are described by a 5-layer heat conductivity soil model and by a hydrological model to determine evaporation and runoff. The model is currently used mainly in two different horizontal resolutions: T21 and T42. The corresponding Gaussian grids for calculating the non-linear and diabatic terms have a resolution of approximately 5.6° and 2.8°, respectively. The model uses 19 vertical layers in a hybrid σ - p -coordinate system. The annual* and diurnal cycles of the solar radiation are included. The annual cycle of the sea surface temperature is prescribed. A comprehensive description of the model ECHAM can be found in Roeckner et al. (1992), which also contains a basic climatology of the model.

In this paper, we analyse two runs at T42 resolution both simulating present day climate. The first run (GAGO) uses the observed SST of the years 1979–1988 as lower boundary. The second run (CTRL) is a so-called control run, i.e., every model year the identical annual cycle of the mean climatological SST is inserted as lower boundary. Two ten-year periods have been selected from this run (years 11–20 and years 21–30). For studying the impact of resolution on the performance of our method and on the blocking frequency, also 10 years of a GAGO simulation (observed SST) performed with ECHAM3 at T21 resolution are analysed.

Finally, a run simulating the climate of an atmosphere with increased atmospheric CO₂ is analysed in order to study the impact of global warming on the blocking frequency. Cubasch et al. (1992) conducted a set of four CO₂ scenario integrations with a coupled atmosphere-ocean general circulation model, each extending over 100 model years. Among those was a control ("1 × CO₂") integration where the atmospheric equivalent CO₂ concentration was kept constant at the present day value, and a Scenario A integration where the

* Each ECHAM model year consists of 12 months, which have an identical length of 30 days.

Table 1. Overview of data inserted into our blocking identification method

Origin of data	Name	Resolution	Time period	Remark
ECMWF analyses	Obs	T42	1982–1989	observations
ECHAM3 model	GAGO	T42	1979–1988	observed SST
ECHAM3 model	CTRL	T42	model years 11–20 model years 21–30	climatological SST
ECHAM3 model	GAGO	T21	1979–1988	observed SST
ECHAM3 model	SCA	T42	model years 13–22 model years 23–32	increased SST

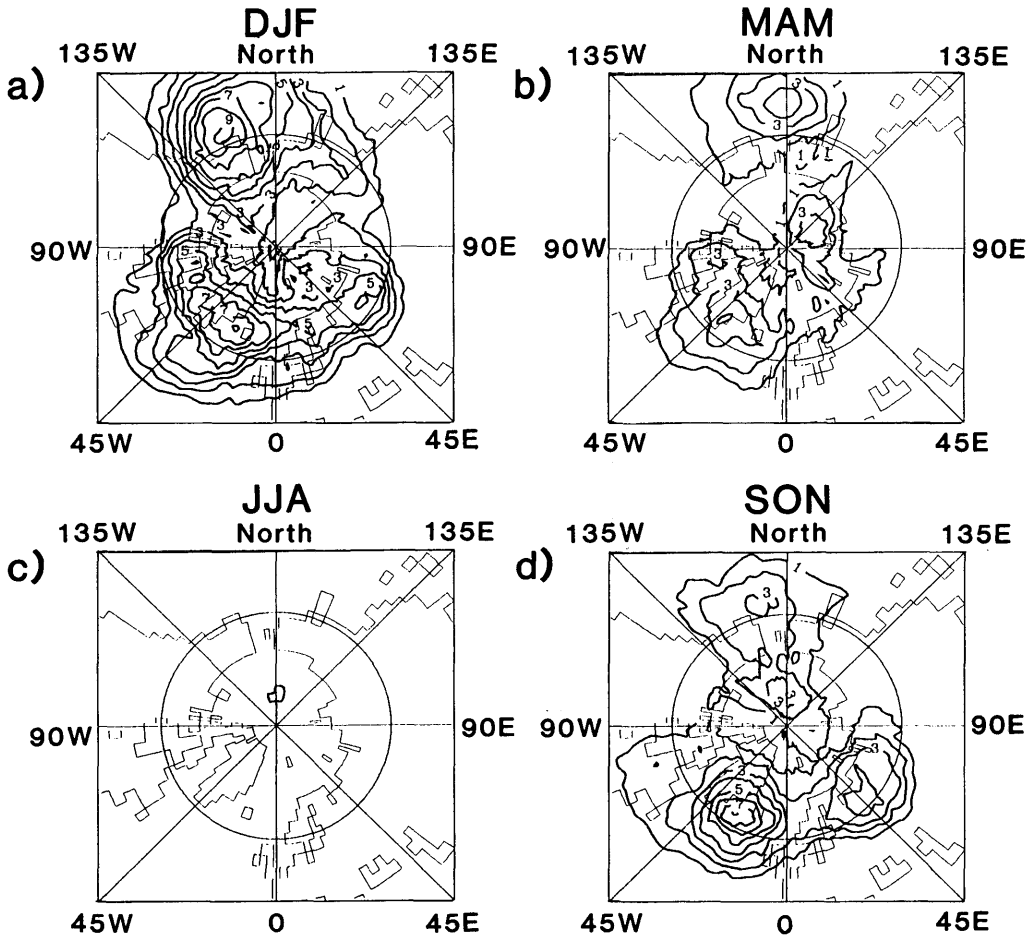


Fig. 4. Northern Hemisphere blocking frequency of ECMWF analyses in T42 resolution from 1982–1989. The contour interval is 1%. (a) DJF, (b) MAM, (c) JJA, (d) SON.

equivalent CO_2 concentration was increased according to IPCC Scenario A (Houghton et al., 1990), which corresponds to an increase of approximately 1.3% per year. From these runs the difference of the SST between Scenario A (mean of years 91–100) and the “ $1 \times \text{CO}_2$ ” integration (mean of years 1–10) was determined. This difference was then added to the climatological sea surface temperature. Using the modified sea surface temperature and the equivalent CO_2 concentration of the coupled Scenario A simulation (mean of the years 91–100), a thirty year integration was performed with the uncoupled atmosphere model ECHAM3/T42 (Perlwitz et al., 1994). This is a kind of a stationary Scenario A experiment (time slice technique). The global mean sea surface temperature of this run is 2.0 K higher on average than in the control simulation. From this simulation two decades (years 13–22 and 23–32) were selected.

3.2. Results

First we applied our method for an objective identification of individual blocking events to the ECMWF analyses (see Table 1). We display the result in terms of blocking frequency in each season for the Northern Hemisphere (Fig. 4). The blocking frequency is determined as the ratio of the number of blocked days (according to our method) to the total number of days.

A three-fold structure is found during winter and in the transitional seasons. We notice a maximum between Greenland and Iceland, which seems to have a rather fixed location throughout the seasons. Further on, a maximum in the North Pacific is identified. Here the anomalies tend to change their mean position from the Aleutians in winter to more westerly longitudes in the transitional seasons. A third frequency maximum can be traced over the Eurasian continent from westerly location in fall to a final point at about 135°E in the Arctic Sea. The highest frequency is attributed to the Pacific blocking events in winter. The major Atlantic blocking season, however, starts earlier in fall. The three maxima were also found by other investigators (Dole and Gordon, 1983; Blackmon et al., 1986). However, their maxima were located a little further to the south. A reason for this discrepancy could be the normalizing of height anomalies by the sine of latitude carried out by these authors. On the other hand the results of Mullen (1987) showed a better agreement with our findings, at least over the Atlantic.

Using our two-dimensional fields of blocking frequency as input, a one-dimensional longitudinal distribution is produced by counting the relative number of days with a blocking event at a certain longitude and at any latitude of the Northern Hemisphere. Fig. 5 (full line) displays the result for the winter. Two distinct maxima show up: one

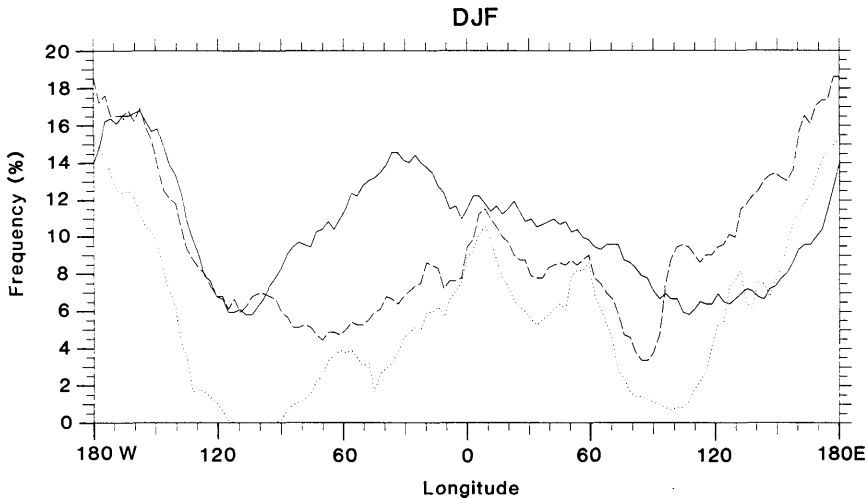


Fig. 5. Longitudinal distribution of blocking frequency in the Northern Hemisphere winter for ECMWF analyses (1982–1989) in T42 resolutions according to our method (full line), compared to the blocking index of Tibaldi and Molteni (1990) of the same data set and period (dotted) and a recent modification of their index (dashed).

above the Pacific and above the Atlantic. The maximum of the Eurasian continent that was visible in Fig. 4 is hardly detectable in the one-dimensional distribution. We also applied the method of Tibaldi and Molteni (1990) and a recent modification of that method (Tibaldi et al., 1993) to the observational data (see also Appendix). These methods generally produce only one-dimensional distributions as the selection criteria are based on meridional gradients or anomalies at given latitudes. The results of both methods are also plotted in Fig. 5. By the way of its construction the modified method of Tibaldi et al. yields higher frequencies of blocking than the old method of Tibaldi and Molteni. In comparison

to our method, the procedures of Tibaldi and collaborators yield higher frequencies above the Pacific and lower frequencies above the Atlantic. Their Pacific maximum is found approximately 30° west of our maximum. The Tibaldi et al. (1993) method yields a maximum above Europe while our method produces its maximum at 40° W above the Atlantic Ocean.

After the demonstration of the performance of our blocking identification method for observational data, we will use the method in order to validate the atmosphere general circulation model ECHAM3. To this end, we analyse the model output from a GAGO run performed with T42 resolution and with prescribed SST of years 1979–1988

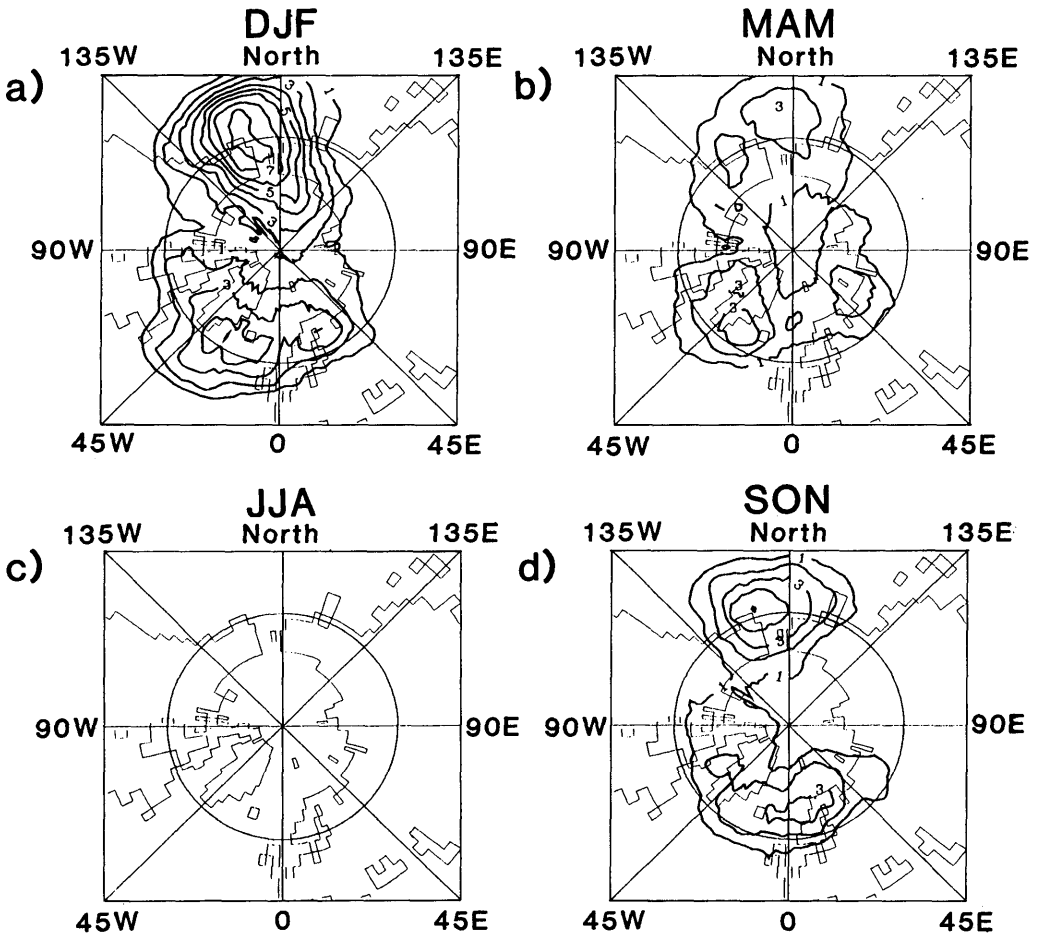


Fig. 6. Same as Fig. 4, but for a ECHAM3/T42 simulation forced by observed SST from 1979–1988.

(see also Table 1). The blocking frequency is shown in Fig. 6 for the Northern Hemisphere. At first sight, the absence of the Eurasian maximum is noticed (cf. Fig. 4). In comparison to observations, the frequency above the North Atlantic is realistically reproduced. The Pacific blocking cases appear further north than in the observations. Nevertheless, the frequency is similar to the observed one.

The lifetime of the selected positive anomalies is investigated for analyses (ECMWF) and model output (ECHAM3/T42, CTRL run) for the Northern Hemisphere (Fig. 7). To this end we applied our routine for different time thresholds: 1, 2, 3, 4, 5, ... days. From this cumulative distribution the statistics of Fig. 7 is obtained by calculation of differences. The distribution of observations shows a relative maximum of occurrence with a lifetime of 5 days. This value backs up the selection of the duration threshold in our objective identification procedure. On the other hand the model results do not have this intimated bimodal structure, the frequencies rather follow a binomial distribution.

The performance of different model runs in the Northern Hemisphere is further illustrated by the longitudinal distribution of the blocking frequency. A comparison of ECMWF analyses (years

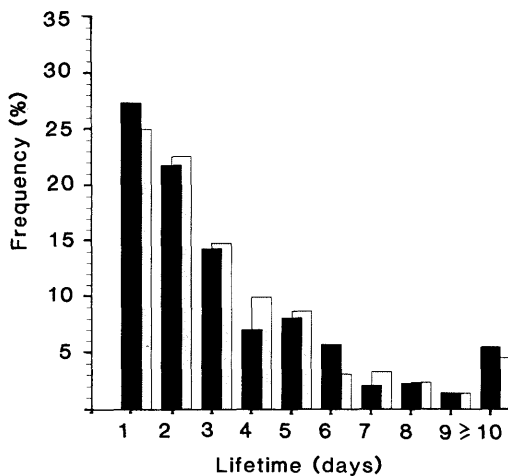


Fig. 7. Percentage of Northern Hemisphere positive anomalies of geopotential height in 500 hPa of a certain lifetime for ECMWF analyses (full columns) and ECHAM model (shaded columns). For the model half-day time steps are added to the next higher full day.

1982–1989) and several ECHAM3 model runs at T42 horizontal resolution is presented in Fig. 8. In addition to the 10 year GAGO run (observed SST the years 1979–1988), which has already been analysed above, two ten-year periods of a control run (climatological SST) with ECHAM3/T42 (see also Table 1) are compiled. The two integration periods of the control run show a rather diverse behaviour above the Atlantic in winter and above Northern Europe and Siberia in fall and winter. A high variability in this sector has also been noticed for observations in different decades (Tibaldi, personal communication). The difference between the two integration periods provides an idea of the interdecadal variability of the blocking frequency which has to be considered if discussing the difference between model and observation. In view of this, the difference between the control integrations and the GAGO run is not significant. Also, the discrepancies between model simulation and observation are not very pronounced, though a tendency of the model to underestimate the observations can be observed.

The impact of resolution is studied by comparing a 10-year GAGO run performed with ECHAM3 in T21 horizontal resolution with the GAGO run and a 10-year period of the control run, both performed with T42 resolution (Fig. 9). The impact of resolution is weak and of a similar size as the difference between two ECHAM3/T42 control simulations for different periods (Fig. 8).

As a final example, we study the impact of global warming on the blocking frequency. To this end we compare two ten-year periods of a ECHAM3/T42 control integration (present day climatological SST) with two 10-year periods of a Scenario A time slice integration (modified SST), all performed with ECHAM3 (see also Table 1, and Subsection 3.1).

In general, the one-dimensional longitudinal distributions of the blocking frequency in the Northern Hemisphere winter (Fig. 10) show no substantial frequency change due to global warming, the changes being of the same order as the differences between different periods of the same run. The increase of the Pacific frequency maximum in winter indicates the occurrence of seasonal shifts in the distribution as in fall a corresponding decrease is found (see also Fig. 11). The hemispheric fields of the differences of the frequency distributions between the two 10-year

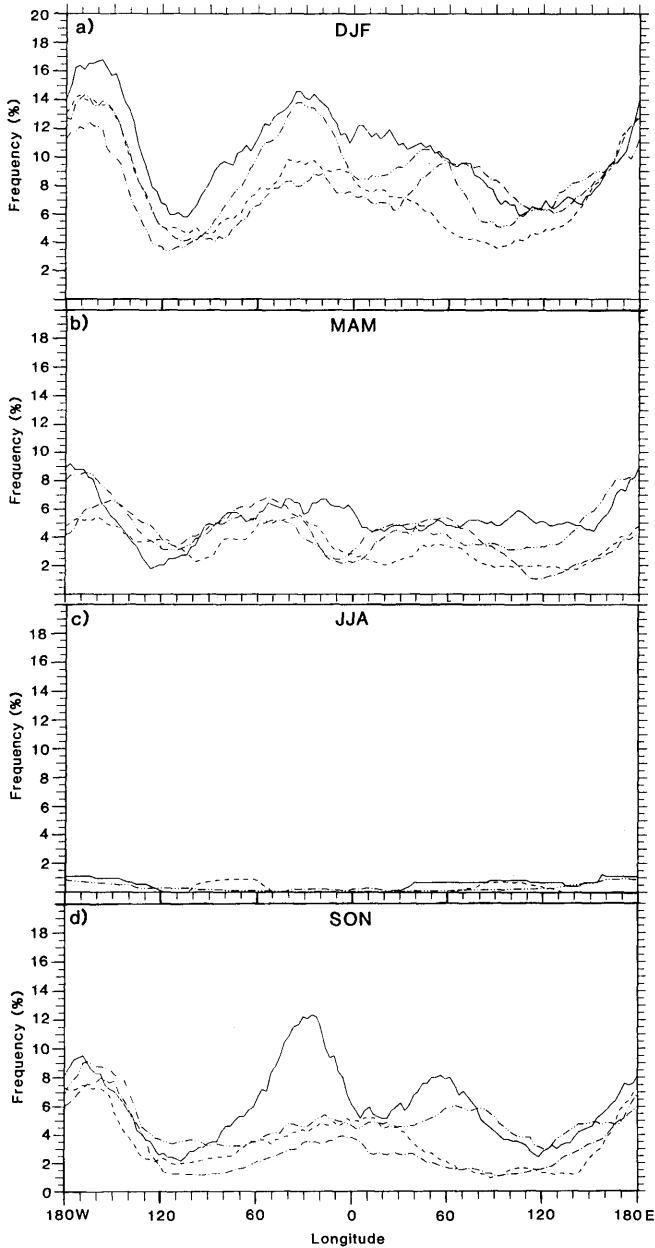


Fig. 8. Longitudinal distribution of blocking frequency in the Northern Hemisphere, for: ECMWF analyses in T42 resolution from 1982–1989 (—); ECHAM3/T42 control run, years 11–20 (---); ECHAM3/T42 control run, years 21–30 (-·-·-); ECHAM3/T42 GAGO-run (SST 1979–1988) (-----); (a) DJF, (b) MAM, (c) JJA, (d) SON.

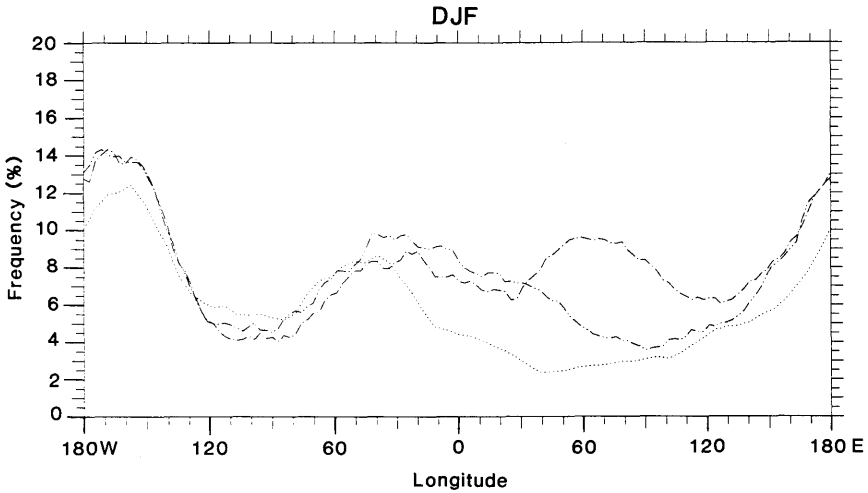


Fig. 9. Longitudinal distribution of blocking frequency in the Northern Hemisphere during winter (DJF) for: ECHAM3/T21 GAGO run (SST 1970–1988) (.....); ECHAM3/T42 control run, years 11–20 (-----); ECHAM3/T42 GAGO run (SST 1970–1988) (-·-·-·-).

integrations of Scenario A and the control run are presented in Fig. 11 for Northern Hemisphere. A seasonal shift of the frequency maximum in the Atlantic sector is noticed. In winter the blocking frequency increases with global warming. In spring and fall higher frequencies are found in the control run. A similar behaviour with blocking frequency

of the control run exceeding Scenario A is found above the Aleutians in fall. In the warmer climate the major frequency of blocking is concentrated in winter, whereas a reduction is noticed in autumn.

Bates and Meehl (1986) analysed the response of blocking frequency to CO₂ doubling. Their winter signal (their Fig. 8) is different from our response.

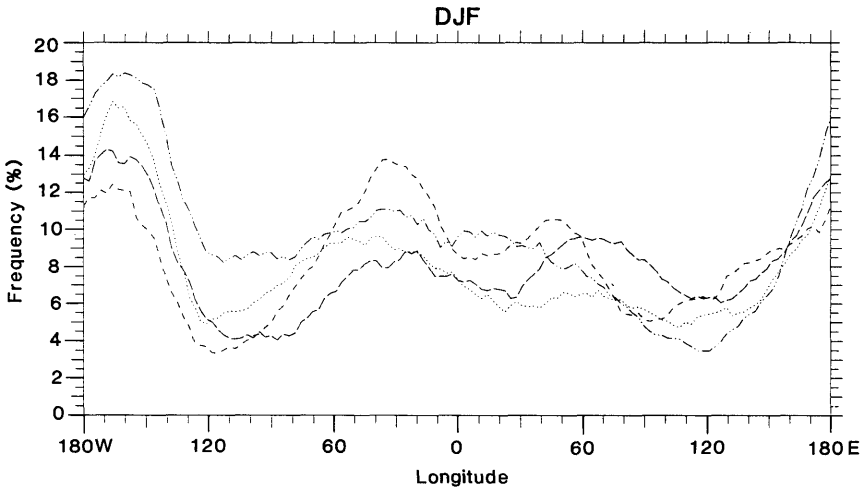


Fig. 10. Same as Fig. 9, but for: ECHAM3/T42 control run, years 11–20 (—); ECHAM3/T42 control run, years 21–30 (-----); ECHAM3/T42 Scenario A run, years 13–22 (.....); ECHAM3/T42 Scenario A run, years 23–32 (-·-·-·-).

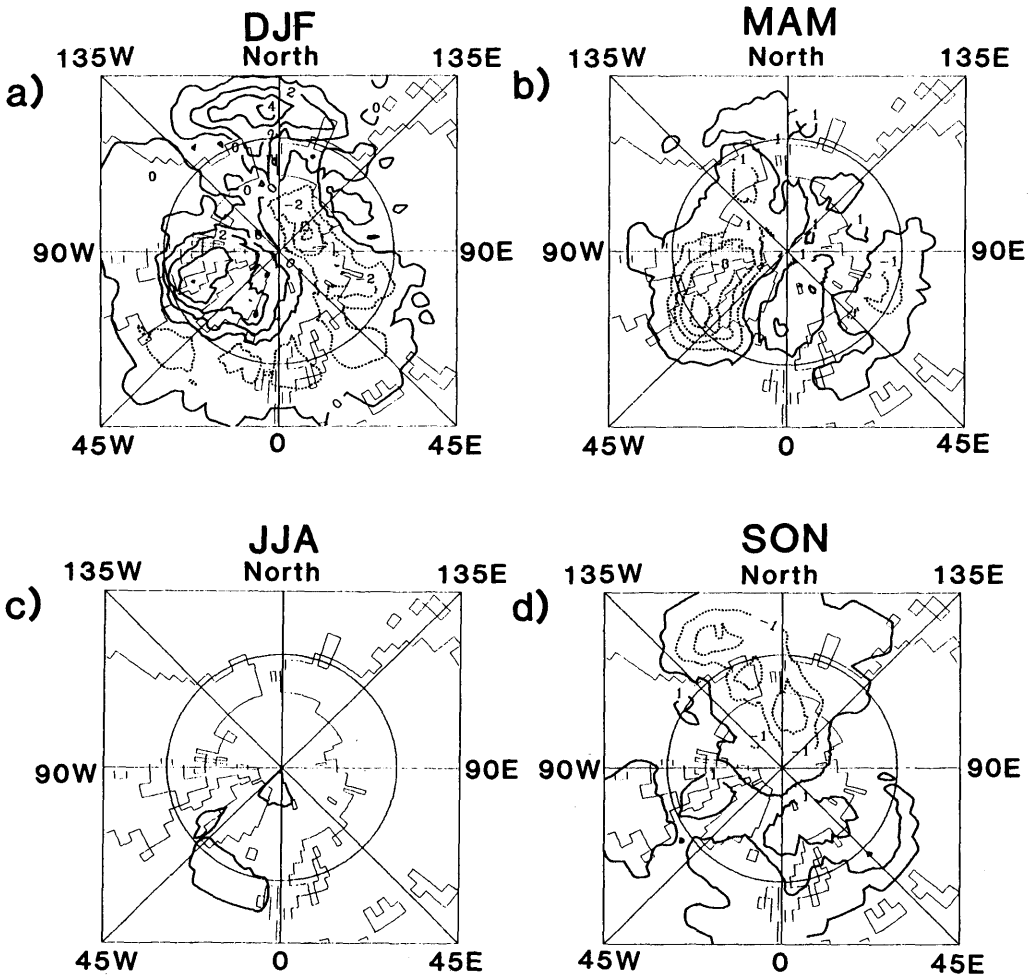


Fig. 11. Difference of blocking frequency between ECHAM/T42 Scenario A run (mean of years 11–20) and reference run (mean of years 11–20) for Northern Hemisphere, (a) DJF, (b) MAM, (c) JJA, (d) SON. The contour interval is 1%. Negative contours are dotted.

In the Pacific sector they detected a westward shift of the maximum, but no intensification as we do. In the Atlantic sector they found an intensification, which more resembles our result. However, in view of the rather high interdecadal variability of the signal, it is hard to judge whether the differences in the Pacific sector are due to internal variability or due to real differences in the global warming signal as simulated by two different models. To some extent the differences can also be attributed to differences in the blocking definition which was applied.

4. Conclusion

We have presented a new objective procedure for blocking identification which copes with the problems of the gradual shift of blockings, of varying extension and lifetime, and of applicability to different grid resolution. The method allows the identification of individual blocking events. It does not require the preselection of certain sectors or of a latitude where blocking is predominantly found. This allows the use of the method also for analysing global change simulations.

For our method the time series of geopotential height at 500 hPa was detrended and the seasonal cycle was eliminated. Then contiguous areas in the three-dimensional longitude–latitude–time domain were selected, where the anomaly exceeds a certain threshold for at least 5 days.

With these criteria, a Northern Hemisphere blocking climatology is evaluated from ECMWF analyses of the years 1982–1989. Three centers of action are identified: above the Aleutians, west of Iceland, and above Western Siberia. The distribution found with our method is rather similar to the results of other investigations, particularly to the blocking index of Tibaldi and Molteni (1990) and a recent modification of this index (Tibaldi et al., 1993). The major blocking regions are coincidentally identified. However, our method places the Atlantic maximum about 30° to the west, and the Pacific maximum slightly to the east. The frequency maximum above the Atlantic is higher, while the number of Pacific blockings is smaller than the index of Tibaldi and collaborators suggests. It can be inferred that our method succeeds in identifying persistent anomalies which are hidden by the mean field.

We applied our method for the identification of individual blocking events in order to investigate the performance of the atmosphere general circulation model ECHAM3 with respect to blocking events. At T42 horizontal resolution, ECHAM3 simulates a fairly realistic Northern Hemisphere blocking distribution. In a warmer Scenario A climate, a seasonal shift of the frequency distribution is simulated.

Finally, we would like to mention that merely by analysing $-z_{500}$ instead of the 500 hPa geopotential height z_{500} also persisting intense lows (cut-off lows) can be identified. Using our identification method for blocking highs and for cut-off lows Ponater et al. (1994) were able to show that in case of a strong negative “Atlantic Oscillation” index, where the Icelandic low is weak, the blocking frequency is enhanced in the North Atlantic region and negative anomalies never occur. In the case of a strong positive “Atlantic Oscillation” index, i.e., in the case with an anomalous strong Icelandic low, there is a tendency towards the formation of negative anomalies in the same region, while blocking occurs quite rarely. Here our technique can provide more information about the characteristics of a given flow pattern than

conventional low-pass filtering analysis that does not distinguish between positive and negative persistent anomalies.

5. Acknowledgements

This research was supported by the commission of the European Communities through grant EPOC-0003-C(MB), by the German Federal Ministry of Research and Technology (BMFT) through grant 07 KFT 056 and by the Deutsche Forschungsgemeinschaft within division SFB 318. Thanks are to Dr. Stefano Tibaldi and Dr. Emilio Tosi, both at the University of Bologna, for several fruitful discussions, and to Dr. Tibaldi also for placing his blocking indices to our disposal. The authors would also like to thank Dipl.-Met. Jan Perlwitz for providing the 500 hPa geopotential height field of the ECHAM3/T42 Scenario A simulation, and Dr. Michael Ponater for helpful discussion.

6. Appendix

Tibaldi and his collaborators developed several simple measures to estimate blocking frequency from grid point fields of geopotential height in 500 hPa. We present two blocking ideas of these authors, which are compared to our method. The indices were designed for 4° by 4° resolution. We applied the method for the smaller resolution of T42.

6.1. Old blocking index (Tibaldi and Molteni)

This definition (Tibaldi and Molteni, 1990) is essentially derived from the work of Lejenäs and Økland (1983), to which the reader is referred for a more extensive justification of the criteria. The procedure the authors have applied is as follows: the 500 hPa field is firstly evaluated on a 4° by 4° regular latitude–longitude grid covering the Northern Hemisphere. Then the geopotential gradients GHGS and GHGN (referring to middle and high latitudes respectively) are computed for each longitude point of the grid:

$$\text{GHGS} = \frac{z(\phi_0) - z(\phi_s)}{(\phi_0 - \phi_s)},$$

$$\text{GHGN} = \frac{z(\phi_N) - z(\phi_0)}{(\phi_N - \phi_0)},$$

where:

$$\phi_N = 80^\circ \text{N} + \Delta,$$

$$\phi_0 = 60^\circ \text{N} + \Delta,$$

$$\phi_s = 40^\circ \text{N} + \Delta,$$

$$\Delta = -4^\circ, 0^\circ, +4^\circ.$$

A given longitude is then defined as "blocked" at a specific instant in time if the following conditions are satisfied for at least one value of Δ .

- (1) GHGS > 0,
- (2) GHGN < -10 m/deg lat.

6.2. New blocking index (Tibaldi–Molteni–Ruti–Maruca)

This blocking index (Tibaldi et al., 1993) has a complex structure, because it involves both the use of meridional gradient of geopotential height and its anomaly; the index was tuned to work in two particular areas in the Northern Hemisphere, namely the Euro-Atlantic area (30.00°W–33.75°E) and the Pacific one (165.35°E–146.25°W). It is an extension of the original index of Tibaldi and Molteni (1990). In order to identify a blocking situation we require that:

$$(\text{GHGS} > 0. \text{AND.} \text{GHGN} < -10.2 \text{ m}/(\text{deg lat.}))$$

$$. \text{AND.} \text{ANOM}(69^\circ) > 40 \text{ m}$$

$$. \text{OR.} \text{ANOM}(69^\circ) > 230 \text{ m}$$

(for the Euro-Atlantic sector)

$$(\text{GHGS} > 0. \text{AND.} \text{GHGN} < -9.5 \text{ m}/(\text{deg lat.}))$$

$$. \text{AND.} \text{ANOM}(69^\circ) > 35 \text{ m}$$

$$. \text{OR.} \text{ANOM}(69^\circ) > 150 \text{ m}$$

(for the Pacific sector)

where

$$\text{GHGS} = \frac{z(\phi_0) - z(\phi_s)}{(\phi_0 - \phi_s)},$$

$$\text{GHGN} = \frac{z(\phi_N) - z(\phi_n)}{(\phi_N - \phi_n)},$$

$$\text{ANOM} = z^p - \bar{z}^p,$$

$$\bar{z}^p = \frac{1}{M} \sum_{t=1}^M z^p (\text{lon., lat.}),$$

p = winterpentad,

$$\phi_N = 86^\circ \text{N},$$

$$\phi_n = 75^\circ \text{N},$$

$$\phi_0 = 60^\circ \text{N} + \Delta,$$

$$\phi_s = 40^\circ \text{N} + \Delta,$$

$$\Delta = -4^\circ, 0^\circ, +4^\circ (\text{Euro-Atl.}),$$

$$\Delta = -8^\circ, -4^\circ, 0^\circ, +4^\circ, +8^\circ (\text{Pacific}),$$

M = number of winter pentads

within considered time period.

The geopotential height gradient is calculated between modified latitudinal limits in respect to those used by Tibaldi and Molteni, in order to achieve a better identification of blocking situation in the northern part of the hemisphere.

The .OR.ANOM(69°N) > condition is also used to improve the index capability to identify atmospheric blocking when their position is more northern than usual. The .AND.ANOM(69°N) > condition is used to avoid the identification of a cut-off low situation as a blocking.

REFERENCES

- Bates, G. T. and Meehl, G. A. 1986. The effect of CO₂ concentration on the frequency of blocking in general circulation model coupled to a simple mixed layer ocean model. *Mon. Wea. Rev.* **114**, 687–701.
- Baur, F. 1958. Die jahreszeitliche und geographische Verteilung der blockierenden Hochdruckgebiete auf der Nordhalbkugel nördlich des 50. Breitengrades im Zeitraum 1949–1957. *Idöjaras* **62**, 73–81.
- Bengtsson, L. 1981. Numerical prediction of atmospheric blocking: A case study. *Tellus* **33**, 19–42.
- Blackmon, M. L., Mullen, S. L. and Bates, G. T. 1986. The climatology of blocking events in a perpetual January simulation of a spectral general circulation model. *J. Atmos. Sci.* **43**, 1379–1405.
- Brezowsky, H., Flohn, H. and Hess, P. 1951. Some remarks on the climatology of blocking action. *Tellus* **3**, 191–197.
- Charney, J. G., Shukla, J. and Mo, K. C. 1981. Comparison of a barotropic blocking theory with observations. *J. Atmos. Sci.* **38**, 762–779.

- Coughlan, M. J. 1983. A comparative climatology of blocking action in the two hemispheres. *Aust. Met. Mag.* **31**, 3–11.
- Cubasch, U., Hasselmann, K., Hck, H., Maier-Reimer, E., Mikolajewicz, U., Santer, B. D. and Sausen, R. 1992. Time-dependent greenhouse warming computations with a coupled ocean-atmosphere model. *Climate Dyn.* **8**, 55–69.
- Dole, R. M. and Gordon, N. D. 1983. Persistent anomalies of the extratropical Northern Hemisphere wintertime circulation: geographical distribution and regional persistence characteristics. *Mon. Wea. Rev.* **111**, 1567–1586.
- Elliott, R. D. and Smith, T. B. 1949. A study of the effects of large blocking highs on general circulation in the northern hemisphere westerlies. *J. Meteorol.* **6**, 67–85.
- Hartmann, D. H. and Ghan, S. J. 1980. A statistical study of the dynamics of blocking. *Mon. Wea. Rev.* **108**, 1144–1159.
- Houghton, J. T., Jenkins, G. J. and Ephraums, J. J. (eds.), 1990. *Climate change, the IPCC scientific assessment*. Cambridge University Press, Cambridge, 365 pp.
- Knox, J. L. and Hay, J. E. 1984. Blocking signatures in the Northern Hemisphere: Rationale and identification. *Atmosphere-Ocean* **22**, 36–47.
- Lejenäs, H. and Økland, H. 1983. Characteristics of Northern Hemisphere blocking as determined from a long time series of observational data. *Tellus* **35A**, 350–362.
- Mullen, S. L. 1986. The local balances of vorticity and heat for blocking anticyclones in a spectral general circulation model. *J. Atmos. Sci.* **43**, 1406–1441.
- Mullen, S. L. 1987. Transient eddy forcing of blocking flows. *J. Atmos. Sci.* **44**, 3–22.
- Noar, P. F. 1983. Numerical modelling of blocking, with reference to June 1982. *Aust. Met. Mag.* **31**, 37–49.
- Perlwitz, J., Cubasch, U. and Roeckner, E. 1994. Simulation of greenhouse warming the ECHAM-3 model using the time-slice method. In G. J. Boer (ed.): *Research activities in atmospheric and oceanic modelling, CAS/JSC Working Group on Numerical Experimentation, Report no. 19*. WMO/TD-No. 592, 9.3–9.4.
- Ponater, M., König, W., Sausen, R. and Sielmann, F. 1994. Circulation regime fluctuations and their effect on intraseasonal variability in the ECHAM climate model. *Tellus* **46A**, 265–285.
- Rex, D. P. 1950. Blocking action in the middle troposphere and its effect upon regional climate (II). The climatology of blocking actions. *Tellus* **2**, 275–301.
- Roeckner, E., Arpe, K., Bengtsson, L., Brinkop, S., Dümenil, L., Esch, M., Kirk, E., Lunkeit, F., Ponater, M., Rockel, B., Sausen, R., Schlese, U., Schubert, S. and Windelband, M. 1992. *Simulation of the present-day climate with the ECHAM model: impact of model physics and resolution*. Max-Planck-Institut für Meteorologie, Report No. 93, Hamburg, Germany, ISSN 0937-1060, 171 pp.
- Shukla, J. and Mo, K. C. 1983. Seasonal and geographical variation of blocking. *Mon. Wea. Rev.* **111**, 388–402.
- Sumner, E. J. 1954. A study of blocking in the Atlantic-European sector of the northern hemisphere. *Quart. J. R. Met. Soc.* **80**, 402.
- Sumner, E. J. 1959. Blocking anticyclones in the Atlantic-European sector of the Northern Hemisphere. *Meteorol. Mag.* **88**, 300–311.
- Tibaldi, S. and Ji, L. R. 1983. On the effect of model resolution on numerical simulation of blocking. *Tellus* **35A**, 28–38.
- Tibaldi, S. and Molteni, F. 1990. On the operational predictability of blocking. *Tellus* **42A**, 343–365.
- Tibaldi, S., Ruti, P., Tosi, E. and Maruca, M. 1993. Operational predictability of winter blocking: an ECMWF update. Proceedings of the ECMWF Seminars on *Validation of forecasts and large-scale simulations over Europe*. Reading, UK, 7–11 September 1992, 91–105.
- Trenberth, K. E. and Mo, K. C. 1985. Blocking in the southern hemisphere. *Mon. Wea. Rev.* **113**, 3–21.